Proceedings of ASME ICNMM2006
4th International Conference on Nanochannels, Microchannels and Minichannels
June 19-21, 2006, Limerick, Ireland

Paper No. ICNMM2006-96134

FRICTION FACTORS AND NUSSELT NUMBERS IN SUPERHYDROPHOBIC MICROCHANNELS

Ryan Enright/Stokes Research Institute, University of Limerick/ryan.enright@ul.ie

Cormac Eason/Stokes Research Institute, University of Limerick/Cormac.eason@ul.ie

Tara Dalton/Stokes Research Institute, University of Limerick/tara.dalton@ul.ie

Marc Hodes/Bell Laboratories, Lucent Technologies/hodes@lucent.com

Paul Kolodner/Bell Laboratories, Lucent Technologies/prk@lucent.com

Tom Krupenkin/ Bell Laboratories, Lucent Technologies /tnk@lucent.com

ABSTRACT

Thermal management is becoming an increasing concern as the electronics industry continues to simultaneously push performance while shrinking the size of devices. Average and local heat fluxes well in excess of 100 W/cm^2 and 1000 W/cm^2, respectively, which are projected for next generation electronics, are driving the widespread development of new technologies to remove heat. Microchannel cooling is one such technology that offers orders of magnitude improvement in heat transfer capabilities while also satisfying the need for a reduced footprint to accommodate ever-shrinking device sizes. One shortfall of microchannel cooling, however, is the large pressure drop associated with pumping liquids through micron-sized channels. Superhydrophobic surfaces combine roughness features with low-energy surface treatments to create materials with substantially decreased wettability and drag resistance in laminar flows and represent a promising technology for reducing microchannel flow resistance. To our knowledge the heat transfer behavior of these surfaces has not been characterized from either a theoretical or experimental framework. Two major factors differentiate heat transfer in a superhydrophobic microchannel compared to a conventional one. First, the local flow field in the working fluid adjacent to a superhydrophobic surface is substantially different from the parabolic velocity profile associated with pressure driven Poiseuille flow in a channel with smooth walls. Secondly, there is an insulating air layer that is trapped within the superhydrophobic surface, which separates the microchannel wall from the working fluid. This air layer gives rise to the low shear-stress region responsible for the reduced flow resistance. In this work we present theoretical flow and heat transfer calculations for the flow of water through a superhydrophobic microchannel that is subject to both symmetric and asymmetric isoflux heating based on the Navier slip model and, also, a novel apparent-slip model, developed here, which accounts for the presence of a recirculating air layer.

INTRODUCTION

The advent of high performance electronics in modern computing has been accompanied by the burden of increasing heat generation. Indeed, average heat fluxes in electronic devices are projected to exceed 100 W/cm^2 within the next five years (ITRS, 2003, Krishnan *et al.*, 2005). Power-dissipation needs of this magnitude are likely to surpass the capabilities of current cooling technology, which is characterized by heat transfer to air cooled heat sinks via conduction and, increasingly, heat pipes. An alternative cooling technology, which has been on the horizon since the early 1980's (Tuckerman & Pease, 1981), is microchannel liquid-cooling. Microchannel liquid-cooling is a promising technology for the thermal management of high power devices because of the exceptionally high heat transfer coefficients achieved with length scales on the order of tens of microns (Tuckerman & Pease, 1981). However, inherent in these small length scales are high flow resistances. This presents a challenge, in terms of heat removal, to achieving flow rates necessary for maintaining electronic-component temperatures below operational limits. Indeed, this requirement has resulted in a proliferation of research into micro pumps capable of fulfilling this requirement (Singhal *et al.*, 2004). Recent studies (Ou *et al.*, 2004, Ou & Rothstein, 2005 and Woolford *et al.*, 2005), however, suggest the possibility of a complimentary approach to achieving suitable flow rates in microchannel heat exchangers using superhydrophobic surfaces.

Superhydrophobic surfaces are renowned because of their unique non-wetting properties. The superhydrophobic effect, which results from a combination of surface roughness and favorable surface chemistry, is well documented and readily explained by the Cassie model of wetting (Cassie). The model asserts that when a water droplet is placed onto a suitably rough and hydrophobic surface it will not penetrate in between roughness elements, but instead sit atop these roughness elements, forming a three phase (gas-liquid-solid) interface. The Cassie model predicts the apparent contact angle formed by a droplet placed on a superhydrophobic surface using measures of the roughness and chemistry of the surface as parameters. The model predicts that very large apparent contact angles ($>160^{\circ}$) are possible and such surfaces have been demonstrated extensively in the literature (Öner and McCarthy, 2000, Krupenkin *et al.*, 2004). Superhydrophobic surfaces are also known to occur naturally and an example of this is the lotus leaf (Blassey, 2003). The study of superhydrophobic surfaces has, recently, become much more tractable due to advances in silicon processing and micro-machining. Precise control over surface-roughness geometry is now allowing systematic studies to be undertaken and paving the way for new ideas on how to utilize the unique properties of these surfaces.

Of particular interest is how to employ such surfaces in microchannel cooling. Recent studies have shown that superhydrophobic structures, when utilized in microchannels, have the potential for major laminar-flow drag reduction (Ou *et al.*, 2004, Ou & Rothstein, 2005 and Woolford *et al.*, 2005). The observed drag reduction, in these studies, is postulated to be the result of a three phase interface forming with a substantial area of low-shear air/water interface. This effectively removes the traditional no-slip boundary condition and allows the liquid to demonstrate an apparent slip. The confined air layer on the surface acts like a lubricator for the water flowing over the surface. It should be noted here that in the study of superhydrophobic surfaces the no-slip assumption is never actually violated. (Lauga *et al.*, 2005) The observed phenomenon is not an actual molecular slip and, thusly, is more appropriately known as an apparent slip. Experimental pressure drop reductions approaching 40% have been reported (Ou *et al.*, 2004) and recent numerical simulations suggest that pressure drop reductions of 175% may be possible with optimized surface roughness geometry (Salamon *et al.*, 2005). These simulations have also shown that the Navier slip model can be employed to calculate approximate velocity profiles of flow over a superhydrophobic surface. The Navier slip model (Navier, 1823 as cited in Neto *et al.*, 2005) removes the traditional no-slip boundary condition at the surface and replaces it with a non-zero velocity that is related to the flow velocity gradient at the surface by a linear parameter, known as the slip length. Salamon *et al.* (2005) show how the approximation breaks down at close proximity to the surface where flow interaction with the solid surface occurs. Nonetheless, the concept of slip length remains a very useful empirical parameter.

The use of a superhydrophobic surface as a heat transfer surface is an interesting proposition. The possibility exists for increased heat transfer rates at the liquid-gas interface due to advection. However, this gain could be offset by the presence of the thin lubricating air-layer on the surface, effectively adding a series thermal resistance. This, however, may be acceptable if it can be shown that an overall cooling system efficiency increase may be achieved when energy savings afforded by drag reduction is accounted for. This paper takes the first steps into exploring the heat transfer characteristics of superhydrophobic surfaces from a theoretical vantage. First, the Navier slip hypothesis is employed to derive theoretical friction factors and Nusselt numbers for several wall slip and heating configurations in a parallel plane channel. Then a model is proposed to account for the presence of a recirculating air layer trapped on the superhydrophobic surface with the resultant friction factors and Nusselt numbers being determined.

NOMENCLATURE

A	integration constant
B	integration constant
C_p	constant-pressure specific heat (J/kg.K)
H	channel height (m)
Nu	Nusselt number
Re	Reynold's number
T	temperature (K)
b	slip length (m)
f	Darcy friction factor
h	heat transfer coefficient ($W/m^2.K$)
k	thermal conductivity (W/m.K)
p	pressure (Pa)
q	volumetric flow rate per unit width (m^2/s)
q"	heat flux (W/m^2)
t	gas layer thickness (m)
u	x- direction velocity (m/s)
α	thermal diffusivity, $k/\rho C_p$ (m^2/s)
μ	viscosity (Pa.s)
ρ	density (kg/m^3)
$-_w$	water
$-_a$	air
$-_s$	surface
$-_m$	mean

NAVIER SLIP FLOW

Fully developed, incompressible, flow between parallel planes is considered in the following analysis. The geometry of the solution domain is defined in Figure 1.

Fig. 1 Geometry of the solution domain.

The flow is governed by the Navier-Stokes equations and for this particular case are of the form shown below.

$$\frac{\partial^2 u}{\partial y^2} = \frac{1}{\mu}\left(\frac{dp}{dx}\right) \tag{1}$$

In solving for the flow-field where slip at the wall is present, one must replace the traditional no-slip boundary condition. The Navier slip hypothesis postulates that if slip occurs at a wall boundary then that wall velocity is related to the velocity gradient at the wall by a linear constant of proportionality termed the slip length.

$$u(0) = b\left.\frac{du}{dy}\right|_{y=0} \tag{2}$$

Thus, if we consider the case where both walls exhibit slip then the following boundary conditions may be applied to develop a solution for the velocity profile.

$$u = b\frac{\partial u}{\partial y} \;@\; y = 0 \tag{3}$$

$$\frac{\partial u}{\partial y} = 0 \;@\; y = \frac{H}{2} \tag{4}$$

This results in an expression for the velocity field shown below.

$$u(y) = \left(\frac{dp}{dx}\right)\left(\frac{1}{2\mu}\right)\left(bH + yH - y^2\right) \tag{5}$$

Figure 2, below, depicts a general form of the solution obtained for the velocity profile where two walls exhibit slip.

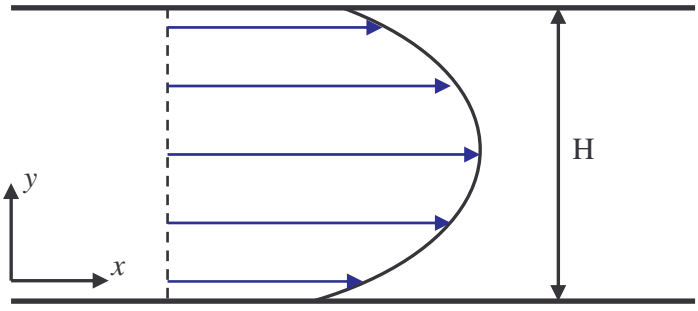

Fig. 2 Two-wall slip velocity profile.

With this knowledge of the velocity profile, one may then calculate the mean velocity and the volumetric flow rate per unit width through a channel exhibiting two-wall slip from the following, respective, equations.

$$u_m = \frac{1}{H}\int_0^H u(y)dy \tag{6}$$

$$q = \int_0^H u(y)dy \tag{7}$$

Thus, the mean velocity and volumetric flow rate per unit width are given by the following expressions.

$$u_m = \left(\frac{dp}{dx}\right)\left(\frac{H}{12\mu}\right)(6b + H) \tag{8}$$

$$q = \left(\frac{dp}{dx}\right)\left(\frac{H^2}{12\mu}\right)(6b + H) \tag{9}$$

Furthermore, one may then calculate the non-dimensional Darcy friction factor[1], which is defined by the equation below.

$$f = \left(\frac{dp}{dx}\right)\left(\frac{4H}{\rho u_m^2}\right) \tag{10}$$

This leads to an expression for the friction factor with two slip walls

$$f = \frac{96\left(\frac{H}{H+6b}\right)}{\mathrm{Re}} \tag{11}$$

where the Reynolds's number, Re, is defined by

$$\mathrm{Re} = \frac{\rho u_m 2H}{\mu} \tag{12}$$

Similarly, if one considers the case where only one wall demonstrates slip the following boundary conditions are applicable.

$$u = 0 \;@\; y = 0 \tag{13}$$

$$u = -b\frac{\partial u}{\partial y} \;@\; y = H \tag{14}$$

The velocity profile is given by

$$u(y) = \left(\frac{dp}{dx}\right)\left(\frac{1}{2\mu}\right)\left(y\left(\frac{H^2 + 2bH}{H+b}\right) - y^2\right) \tag{15}$$

Figure 3, below, depicts a general form of the solution obtained for the velocity profile where one wall exhibits slip.

[1] Known subsequently as the friction factor.

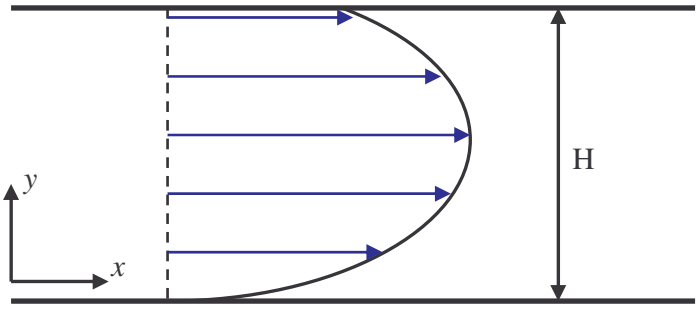

Fig. 3 One-wall slip velocity profile.

The mean velocity and volumetric flow rate per unit width are then given, respectively, by

$$u_m = \left(\frac{dp}{dx}\right)\left(\frac{H^2}{12\mu}\right)\left(\frac{H+4b}{H+b}\right) \tag{16}$$

$$q = \left(\frac{dp}{dx}\right)\left(\frac{H^3}{12\mu}\right)\left(\frac{H+4b}{H+b}\right) \tag{17}$$

The friction factor in a channel where one wall exhibits slip is given by

$$f = \frac{96\left(\frac{H+b}{H+4b}\right)}{\mathrm{Re}} \tag{18}$$

The analytical validity of the derived quantities can subsequently be verified by evaluating the expressions at b = 0, which results in the classical Poiseuille flow theory being returned for fully-developed flow between two, infinite parallel planes. Figure 4, below, illustrates the relationship between the friction factor-Reynold's number product (*f*Re) and the ratio of slip length to channel height (b/H) for the two slip cases investigated. Note that, as the slip length approaches zero, both cases converge on *f*Re=96, which is the typical value for fully-developed flow between two parallel planes.

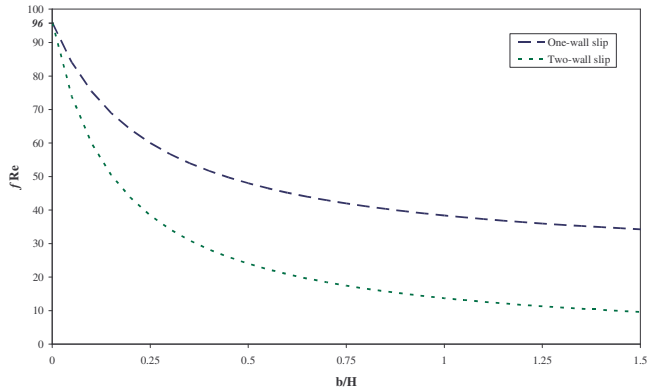

Fig. 4 Non-dimensional plot of frictional pressure losses in parallel plane channels exhibiting slip. *f*Re is the friction factor-Reynold's number product. b/H represents the ratio of slip length to channel height.

NAVIER SLIP HEAT TRANSFER

The analysis is now extended to investigate the implications of the Navier slip hypothesis on fully developed convective flow with constant properties. Two particular cases are examined in detail. First, the case where both walls exhibit slip and have a constant heat flux imposed at the boundaries of the solution domain. The second case examined analyses one wall exhibiting slip with a constant heat flux applied to that boundary. The other wall is modeled with the no-slip boundary condition and is adiabatic. This represents an asymmetric heating condition. Figure 5 defines the two cases investigated.

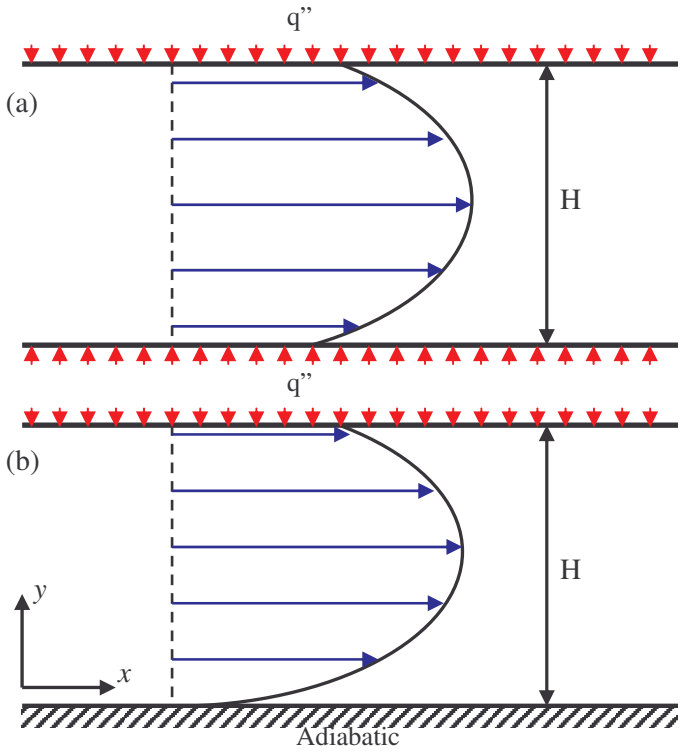

Fig. 5 (a) Case where both walls exhibit slip and are subjected to a symmetric isoflux. (b) Case where one wall exhibits slip and is subjected to an asymmetric isoflux on the slip wall. The other boundary is treated as adiabatic.

The energy equation, neglecting axial conduction, takes the following form

$$\frac{\partial^2 T}{\partial y^2} = \frac{1}{\alpha}u(y)\frac{\partial T}{\partial x} \tag{19}$$

where u(y) is one of the two velocity profiles given above in Eq. 5 and Eq. 15.

Based on the imposed condition of a constant heat flux and thermally fully-developed flow then the following applies (Kays & Crawford, 1993).

$$\frac{\partial T}{\partial x} = \frac{dT_m}{dx} \tag{20}$$

Applying an energy balance to an elemental portion of the flow domain it can then be shown that the following applies.

$$\frac{dT_m}{dx} = \frac{2q_m^{"}}{\rho C_p H u_m} \tag{21}$$

where the average heat flux is defined by

$$q_m^{"} = \frac{1}{2}\left(q_1^{"} + q_2^{"}\right) \tag{22}$$

The following boundary conditions are then imposed in order to solve for the temperature profile in a two-wall slip flow under isoflux heating conditions.

$$T = T_s \ @ \ y = 0 \tag{23}$$

$$\frac{dT}{dy} = 0 \ @ \ y = \frac{H}{2} \tag{24}$$

An expression for the resulting temperature profile is shown below.

$$T(y) = \frac{q^{"}\left(y^4 - 2Hy^3 - 6bHy^2 + H^2(H+6b)y\right)}{H^2(H+6b)k} + T_s \tag{25}$$

Using this knowledge of the temperature profile we can then solve for the mean temperature using the following equation.

$$T_m = \frac{1}{u_m H}\int_0^H u(y)T(y)dy \tag{26}$$

Thus, the mean temperature is given by

$$T_m = \frac{q^{"}H\left(17H^2 + 168bH + 420b^2\right)}{70k(H+6b)^2} + T_s \tag{27}$$

Next, we note the following definitions.

$$q^{"} = h\left(T_s - T_m\right) \tag{28}$$

$$Nu = \frac{h(2H)}{k} \tag{29}$$

Rearranging Equation 27 in the form of Equation 28 and substituting the heat transfer coefficient into Equation 29 we find that the Nusselt number, for two-wall slip flow between parallel planes with an imposed isoflux boundary condition, to be given by the following expression.

$$Nu = \frac{140(H+6b)^2}{17H^2 + 168bH + 420b^2} \tag{30}$$

Scaling the expression non-dimensionally using the parameter b/H we arrive at a general curve for the Nusselt number in a parallel plane geometry with hydrodynamically and thermally fully developed flow (Figure 6). At b/H = 0 it can be seen that Nu = 8.2353, which is expected for the no-slip case in a parallel plane geometry (Rohsenow *et al.*, 1985). Note that as b/H approaches infinity the Nusselt number tends to a value of 12, which represents the case of plug flow.

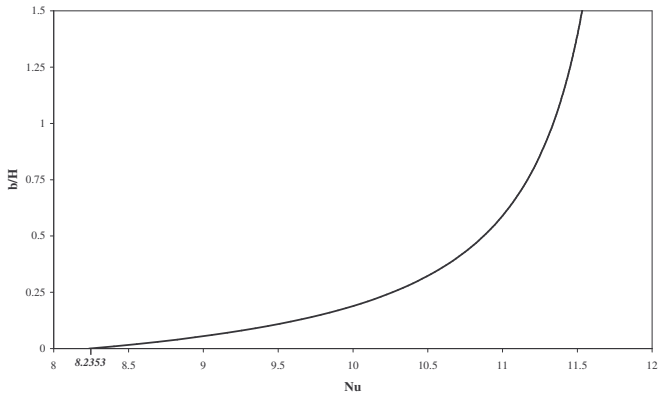

Fig. 6 Non-dimensional plot of b/H to Nusselt number where both walls exhibit slip and are heated symmetrically by an isoflux.

A similar analysis is performed for the case of one-wall slip with a constant heat flux applied to the slip wall. The other wall maintains the classic no-slip boundary condition and is adiabatic. Subsequently the following boundary conditions apply to the analysis.

$$\frac{dT}{dy} = 0 \ @ \ y = 0 \tag{31}$$

$$T = T_s \ @ \ y = H \tag{32}$$

The resulting temperature profile is given by the following equation.

$$T(y) = \frac{q^{"}\left((H+b)y^4 - \left(2H^2 + 4bH\right)y^3 + H^5 + 3bH^4\right)}{H^3(H+4b)k} + T_s \tag{33}$$

We then utilize the above temperature profile to determine the mean temperature shown below.

$$T_m = \frac{q'' 2H\left(13H^2 + 82bH + 132b^2\right)}{35k\left(H + 4b\right)^2} + T_s \qquad (34)$$

Rearranging and substituting as before we arrive at the following expression for the Nusselt number.

$$Nu = \frac{70\left(H + 4b\right)^2}{13H^2 + 82bH + 132b^2} \qquad (35)$$

In Figure 7 we see the general curve of the Nusselt number for the case where one wall exhibits slip and that wall is heated by an isoflux. At b/H = 0 we see that Nu = 5.3846; the typical value for this heating configuration in a parallel plane geometry (Rohsenow *et al.*, 1985). As b/H approaches infinity we see that the limit of the Nusselt number is Nu = 8.4831.

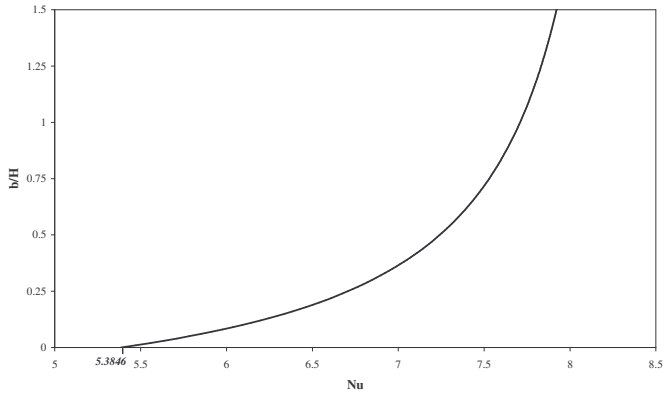

Fig. 7 Non-dimensional plot of b/H to Nusselt number where one wall exhibits slip with asymmetric heating at the slip wall by an isoflux.

RECIRCULATING AIR-LAYER SLIP

In the preceding sections the implications of wall slip were examined by applying the Navier slip boundary condition. However, there are several shortcomings in employing this method to investigate fluid flow in superhydrophobic channels. Firstly, the slip length is not necessarily known *a priori*. Typically this coefficient is determined experimentally (Ou *et al.*, 2004, Ou & Rothstein, 2005 and Woolford *et al.*, 2005) or, as demonstrated recently, via numerical simulations of fluid flow over these surfaces (Salamon *et. al.*, 2005). Another major issue is that the Navier slip model does not account for the fact that superhydrophobic surfaces operate as binary-fluid systems. The thin air layer, which is trapped in and around the roughness elements of the surface, contributes to viscous drag and represents a thermal resistance in the case of heat transfer. Thus the geometry of, and more specifically, the thickness of this air layer will have an impact on both flow and heat transfer through the channel. Presented next is a model which captures the flow physics of this binary fluid system with some idealized conditions. Similar models have been proposed, most notably by Tretheway and Meinhart (2004), to account for apparent slip due to the presence of an air layer or bubbles on a solid surface. This model differs, as it considers the air layer as a closed volume, within which air recirculates. It is believed that this represents a more realistic view of the actual conditions within the air layer. Outside the scope of this present analysis is the impact of the air layer on heat transfer. However, it is believed that a solution for the respective velocity profiles in the gas and liquid domains represents a stepping stone towards that end.

We begin the analysis by stating the assumptions of the proposed model. The case being modeled in this analysis is depicted in Figure 8. All velocity profiles are treated as fully developed and the no-slip boundary condition applies at every solid boundary in the flow. The no-slip condition is also applied to the air/water interface such that the velocity and shear are matched at the interface. Thus, it is postulated that the pressure driven movement of the water induces a recirculating flow in the air layer. Note that this present analysis represents the case where spacing between roughness elements goes to infinity, effectively leaving a bed of air over which the water flows and, thus, gives the maximum possible slip length. Also note that only one superhydrophobic wall is modeled with the other wall modeled as a classic no-slip surface.

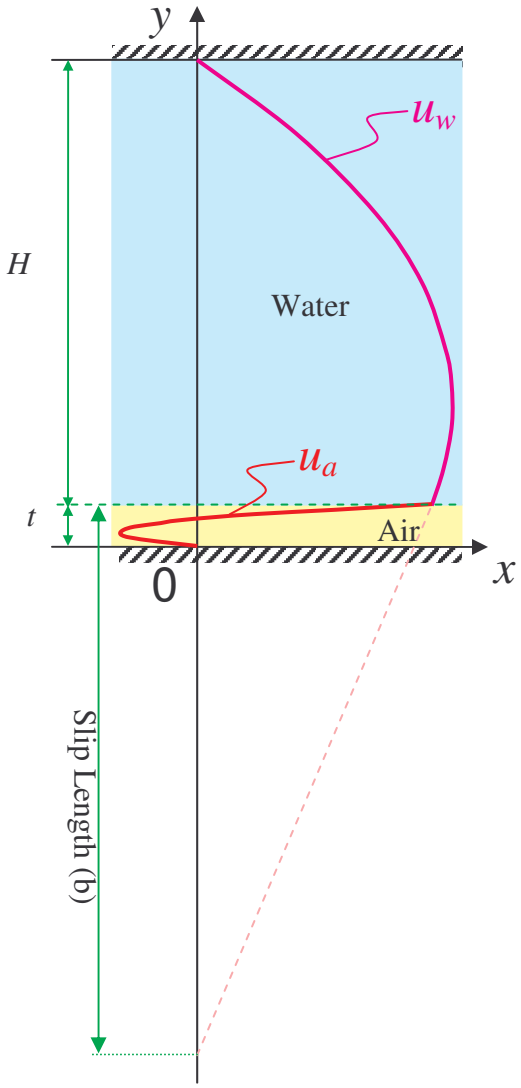

Fig. 8 Apparent-slip flow model with recirculating air layer. Note that the slip length is defined by the Navier slip model.

The governing equations in the water and air layer are, respectively, given below.

$$\frac{\partial^2 u_w}{\partial y^2} = \left(\frac{1}{\mu}\right)\left.\frac{dp}{dx}\right|_w \tag{36}$$

$$\frac{\partial^2 u_a}{\partial y^2} = \left(\frac{1}{\mu}\right)\left.\frac{dp}{dx}\right|_a \tag{37}$$

Note that the pressure drop in the water is prescribed, while that in the air layer is unknown. Integrating twice we arrive at the following forms of the velocity profiles.

$$u_w = \frac{dp_w}{dx}\frac{y^2}{2\mu_w} - \frac{A_w y}{\mu_w} - \frac{B_w}{\mu_w} \tag{38}$$

$$u_a = \frac{dp_a}{dx}\frac{y^2}{2\mu_a} - \frac{A_a y}{\mu_a} - \frac{B_a}{\mu_a} \tag{39}$$

The following boundary conditions (Eqns. 40-43) and constraint (Eqn. 44) are then applied to equations 38 and 39 in order to solve for the constants of integration.

$$u_a = 0 \;@\; y = 0 \tag{40}$$

$$u_w = 0 \;@\; y = H + t \tag{41}$$

$$u_a = u_w \;@\; y = t \tag{42}$$

$$\mu_a \frac{\partial u_a}{\partial y} = \mu \frac{\partial u_w}{\partial y} \;@\; y = t \tag{43}$$

$$\int_0^t u_a dy = 0 \tag{44}$$

Implementation of the boundary conditions and constraint results in a set of simultaneous equations, which are solved yielding the following forms of the velocity profiles in the air and water layers.

$$u_w = \left(\frac{dp}{dx}\right)\frac{(t - H + y)}{2\mu_w\left(-t\mu_w + 8t\mu_a - 4H\mu_a\right)} \text{ x}$$
$$\left(-3t^2\mu_w + 8t^2\mu_a + t\mu_w y + Ht\mu_w - 4Ht\mu_a - 8t\mu_a y + 4H\mu_a y\right) \tag{45}$$

$$u_a = \left(\frac{dp}{dx}\right)\frac{(-H + 2t)^2(-3y + 2t)y}{2t\left(-t\mu_w + 8t\mu_a - 4H\mu_a\right)} \tag{46}$$

An expression for the slip length can then be computed, using knowledge of the water velocity profile, from the definition given in equation 2. From equation 47, below, we see that the apparent slip length is a linear function of the air layer thickness, t, and the ratio of the fluid viscosities. More importantly, the apparent slip length is not a function of the channel height, as was the case with the Navier slip model.

$$b = \frac{t}{4}\frac{\mu_w}{\mu_a} \tag{47}$$

Figure 9 is an example of predicted apparent slip lengths with varying gas layer thickness in a parallel plane channel with one slip wall, where the two fluids are water and air at standard conditions.

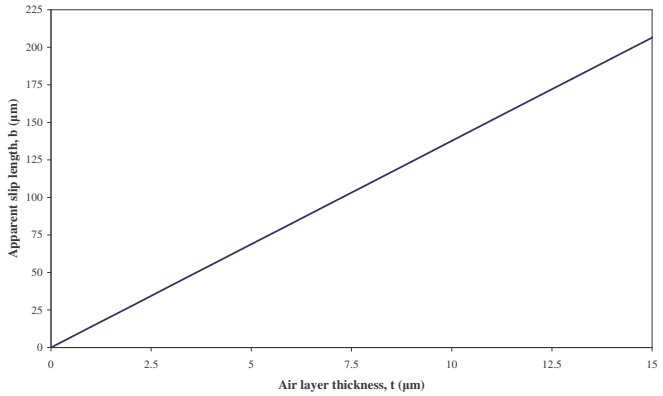

Fig. 9 Predicted apparent-slip lengths with varying gas layer thickness, where the two fluids are water and air at standard conditions.

CONCLUSIONS

An analysis of the theoretical flow and heat transfer in a channel exhibiting slip has been performed employing the Navier slip model. The ratio of the slip length, b, to the height of the channel, H, is seen to have a strong effect on both the friction factor and Nusselt number. As the ratio b/H increases a corresponding decrease is observed in the friction factor, while an increase is seen in the Nusselt number. For the case where both walls exhibit slip and are heated by an isoflux the Nusselt number ranges from 8.2353 at b/H = 0 to an asymptotic value of 12 as b/H tends to infinity. These limits are consistent with typical values expected for the no-slip case and plug flow case, respectively. For the case where one wall exhibits slip with an isoflux, with the other wall no-slip and adiabatic, the Nusselt number ranges from 5.3846 at b/H = 0 to an asymptotic value of 8.4831. The lower limit of this range is consistent with the typical value for the geometry and heating conditions imposed.

An apparent slip model has been developed for a parallel plane channel where one wall exhibits slip, which accounts for a recirculating air layer trapped on the superhydrophobic surface. This model predicts slip lengths which are directly proportional to the thickness of the air layer and are not functions of the channel height. The model is valid for the case where the spacing of the roughness elements tends towards infinity and this can be appreciated as predicted slip lengths from the model are significantly higher than those found in the literature. This suggests that the roughness elements, even when they occupy a small fraction of the superhydrophobic surface, contribute the majority of viscous drag to the flow. As the model provides both velocity profiles for the air and water regions of the flow it is conceivable that the model can be further developed to ascertain the impact of the air layer on heat

transfer from the substrate to the heat transfer fluid and compare this with the predictions made by the Navier slip model concerning heat transfer.

ACKNOWLEDGMENTS

The authors would like to acknowledge the support of the Centre for Telecommunication Value-Chain Research (CTVR).

REFERENCES

Blassey, R., 2003, "Self-cleaning surfaces- virtual realities," *Nature Materials*, **2**, pp. 301-306.

ITRS, 2003. "International Technology Roadmap for Semiconductors (ITRS) 2003," http://public.itrs.net/Files/2003ITRS/Home2003.htm.

Kays, W. M., Crawford, M. E., 1993. *Convective Heat and Mass Transfer* 3rd edn., McGraw-Hill Inc., New York, p.113.

Krishnan, S., Garimella, S. V., Chrysler, G. M. and Mahajan, R. V., 2005. "Towards a Thermal Moore's Law," Proceedings of IPACK 2005, ASME InterPACK '05, July 17-22, San Francisco, California, USA.

Krupenkin, T. N., Taylor, J. A., Schneider, T. M. and Yang, S., 2004, "From Rolling Ball to Complete Wetting: The Dynamic Tuning of Liquids on Nanostructured Surfaces," *Langmuir*, **20**(10), pp. 3824-3827.

Lauga, E., Brenner, M. P. and Stone, H. A., 2005. "Microfluidics:The No-Slip Boundary Condition," to appear as Ch. 15 in *Handbook of Experimental Fluid Dynamics*, eds. Foss, J., Tropea, C. and Yarvin, A..

Navier, C. L. M. H., 1823. "M´emoire sur les lois du mouvement des fluids," *Mem. Acad. Sci. Inst. Fr.*, **6**.

Neto, C., Evans, D. R., Bonaccurso, E., Butt, H. J. and Craig, V. S. J., 2005. "Boundary slip in Newtonian liquids: a review of experimental studies," Rep. Prog. Phys. **68** (2005) 2859-2897.

Öner, D. and McCarthy, T. J., 2000, "Ultrahydrophobic Surfaces. Effects of Topography Length Scales on Wettability," *Langmuir*, **16**, pp. 7777-7782.

Ou, J., Perot, B. and Rothstein, J. P., 2004, "Laminar drag reduction in microchannels using ultrahydrophobic surfaces," *Phys. Fluids*, **16**(12), pp. 4635-4643.

Ou, J. and Rothstein, J. P., 2005. "Direct velocity measurements of the flow past drag-reducing ultrahydrophobic surfaces," *Phys. Fluids*, **17**(10), 103606-(1-10).

Rohsenow, W.M., J.P. Hartnett, E.N. Ganić, (ed.), 1985, Handbook of Heat Transfer Fundamentals, 2nd Edition, McGraw-Hill Book Company.

Singhal, V., Garimella, S. and Raman, A., 2004, "Microscale Pumping Technologies for Microchannel Cooling Systems," *Appl. Mech. Rev*., **57**(3), pp. 191-221.

Tuckerman, D. B. and Pease, R. F. W., 1981. "High performance heat sinking for VLSI," *IEEE Electronic Device Letters*, **2**(5), pp. 126-129.

Woolford, B., Jeffs, K., Maynes, D. and Webb, B. W., 2005. "Laminar fully-developed flow in a microchannel with patterned ultrahydrophobic walls," Proceedings of HT2005, 2005 ASME Summer Heat Transfer Conference, July 17-22, San Francisco, California, USA.